Integrating Observations from MFG and GPM for Near Real Time Heavy Precipitation Monitoring

Mohammd Rafiq and Anoop Kumar Mishra
Centre for Remote Sensing and Geoinformatics, Sathyabama University, Chennai
Email: emidamls6@gmail.com

ABSTRACT

This study deals with merging of high accurate precipitation estimates from Global Precipitation Measurement (GPM) with sampling gap free satellite observations from Meteosat 7 of Meteosat First Generation (MFG) to develop a regional rainfall monitoring algorithm for monitoring precipitation over India and nearby oceanic regions. For this purpose, we derived rainfall signature from Meteosat observations to co-locate it against rainfall from GPM. A relationship is then established between rainfall and rainfall signature using observations from various rainy seasons. Relationship thus derived can be used to monitor precipitation over India and nearby oceanic regions. Performance of this technique was tested against rain gauges and global precipitation products including the Global Satellite Mapping of Precipitation (GSMaP), Climate Prediction Centre MORPHing (CMORPH), Precipitation Estimation from Remote Sensing Information using Artificial Neural Network (PERSIANN) and Integrated Multi-satellitE Retrievals for GPM (IMERG). A case study is presented here to examine the performance of developed algorithm for monitoring heavy rainfall during flood event of Tamil Nadu in 2015.

Keywords: *Near Real Time, GSMap, Meteosat, GPM, Rain gauge, Flood and Drought.*

1. Introduction

Near Real Time (NRT) precipitation information at fine resolution is required to monitor flash floods. Unfortunately Indian region has poor density of ground based rain gauges and Radars. Moreover, usually rain gauge stations stop functioning during severe flood situatuions (Mishra, 2015). Flood events are associated with a large spatial and temporal variation of rainfall and hence continuous NRT high resolution hourly satellite data is essential to monitor such events (Mishra and Srinivasan, 2013). Such observations can be achieved by merging microwave precipitation estimates with rain signatures from geostationary satellites. Past researches report that cold observations from IR are associated with convective clouds and thus heavy precipitation (Mishra et al. 2010; Mishra 2013). In the past few decades, various satellite precipitation products have become widely available for users. These data sets integrate precipitation estimates and signatures from different sensors and satellites into a precipitation product. These data sets include the Tropical Rainfall Measuring Mission Mission (TRMM) Multisatellite Precipitation Analysis (TMPA) NRT product (Huffman et al., 2007), the Global Satellite Mapping of Precipitation (GSMaP) (Kubota et al., 2007; Aonashi et al., 2009), Climate Prediction Centre MORPHing (CMORPH) (Joyce et al. 2004), Precipitation Estimation from Remote Sensing Information using Artificial Neural Network (PERSIANN) (Hsu et al. 1997), Hydro-Estimator (H-E) (Scofield and Kuligowski, 2003), and Integrated Multi-satellitE Retrievals for GPM (IMERG) (Huffman et al. 2015). Validation results show that most of these products have large errors over Indian region (Mishra et al. 2010; Mishra 2013). Mishra et al. (2009a) reported that regional rain signatures derived for India outperform global rainfall signatures for their application over India. Few efforts have been made to monitor rainfall over India and nearby region by synergistic use of multi-satellite sensors (Mishra et al. 2009b, 2010; Mishra et al. 2011a, b; Mishra, 2012; Mishra, 2013). Availability of microwave measurements with broader swath and high frequency ice scattering channels from GPM provide a unique opportunity to merge accurate microwave rainfall information with Infrared observations from Meteosat over India (Rafiq and Mishra, 2018a,2018b, Mishra and Rafiq 2017). The GPM Core Observatory measures precipitation using two sensors: the GPM Microwave Imager (GMI) and the Dual-frequency Precipitation Radar (DPR). A recent preliminary study reports that rainfall estimates from DPR onboard GPM are closer to the gauge estimates than those from PR onboard TRMM (Iguchi et al. 2009).

In this study, we have merged observations from combined DPR and GMI with Meteosat to monitor near real time precipitation over Indian region and nearby ocean. Validations have been performed using rain gauge based product to test the accuracy of the present approach for its application in heavy rainfall cases.

2. Data Used and Study Area

For the present study, Meteosat 7 data of Meteosat First Generation (MFG) are used. MFG provides images of the full Earth disc, and data for weather forecasts. Meteosat provides observations in Thermal Infra Red (TIR) and Water Vapor (WV) absorption band at half-hourly interval, with a spatial resolution of 4 km. Combined GMI-DPR based rainfall from GPM is also used in this study. This product is described by Grecu et al., (2009; 2016). In order to test the performance of present technique, rainfall estimates from GSMaP, CMORPH, PERSIANN and IMERG has also been used in the present technique. Rain gauge observations from AWS is used to validate the performance of present technique. Study area spans from 10ºS-40ºN to 60Eº-100Eº.

3. Methodology

Multi-frequency observations at multiple channels from Meteosat were used to filter out false rainfall signatures. We used a cloud classification scheme devised by Roca et al. (2002) and adopted by Mishra et al. (2010) to delineate non rainy thin cirrus clouds. If brightness temperature in IR band (IRTB)>=270K and cloudy and brightness temperature in WV band (WVTB)<=246K then pixel represents thin cirrus clouds and is screened out. During day time, cloud microphysical properties at near IR observations and visible reflectance were used to screen in rainy pixels following criteria used by Rosenfeld and Gutman (1994).

It was reported by Mishra et al. (2010) that few cirrus clouds were still undetected even after applying threshold based cloud classification. In order to screen out the non rainy cirrus clouds, we used a criteria developed by Adler and Negri (1988) as a second step. Following this approach, a slope (*S*) and a temperature gradient (*Gt*) were estimated for each local temperature minimum (using brightness temperature (IRTB) at 11.5 µm). The terms G_t and S are computed by Eq. (1) and Eq. (2), respectively:

$$G_t = IRTB_{avg} - IRTB_{min} \quad (1)$$

$$S = 0.568(IRTB_{min}-217) \quad (2)$$

Where $IRTB_{min}$ is the local minimum, and as in Adler and Negri (1988), $IRTB_{avg}$ is the mean temperature. It may be noted that local minima is computed for an area covered by 6 IR pixels (4 pixels along the scan and 2 pixels across the scan). A large G_t shows convective clouds; a small G_t represents a weak gradient and shows the presence of cirrus clouds within the window. All pixels having G_t less than S are classified as cirrus clouds and therefore are rejected as non-raining clouds.

Following filtering out erroneous clouds, IRTB were co-located against combined GMI-DPR rainfall within 15 minutes of difference in which auto covariance function of rainfall reduces to about 0.9 (Laughlin, 1981). "15 minutes of difference" is the maximum allowed time difference in simultaneous observations of GPM and Meteosat. Data re-sampling scheme is used to minimize the uncertainty in co-location due to difference in resolution. For the co-location process, rainfall from GPM is remapped at 0.1º grid. Now IR-Observations from Meteosat is also remapped at 0.1º grid. Co-location process is similar as described in Mishra et al. (2010). It may be noted that present algorithm aims to estimate rainfall at 0.1º grid.

For the co-location purpose, 18654 data points (re-sampled at 0.1º grid) consisting of rain events during the years 2015 and 2016 were used. Out of 18654 data points, 6642 were rainy pixels while 12012 were no rainy pixels. A total number of 12862 were used for the independent validation purpose. This shows that out of 31515 (18654+12862) data points 41% of total data points were used for the validation purpose.

Relationship between IRTB and rainfall is shown in Figure 1a. It can be seen that heavy rainfall events are associated with cold brightness temperature representing convective and deep convective clouds. Good

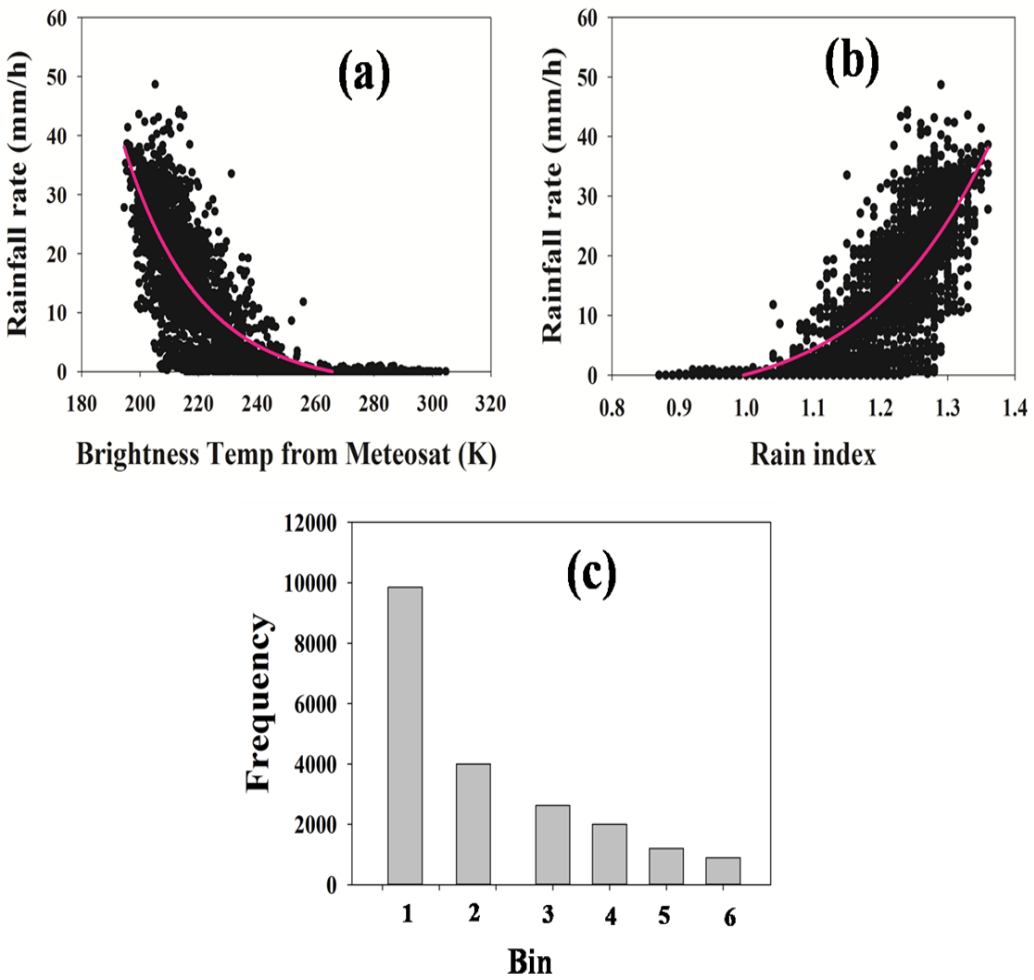

Figure 1: Scatter plot between rainfall rate (from GPM) and (a) brightness temperature (from Meteosat) (b) and rain index. (c) Histogram of frequency at different bins. Precipitation bins are defined as 2 mm/h, 8 mm/h, 15 mm/h, 20 mm/h, 25 mm/h and 30 mm/h (Selected Bin sizes set to accommodate the entire rainfall spectrum)

correlation between rainfall and IRTB may be attributed to the inclusion of good number of heavy rainfall events (convective) and delineation of erroneous cirrus clouds.

A non rainy threshold of about 264K ($IRTB_0$) is observed. We define rain index (RI) as follows:

$$RI = (IRTB_0/IRTB) \quad (3)$$

IRTB>264K indicates RI<1 and is a representative of non rainy cases. Higher values of RI shows heavy rainfall associated with intense rainy systems. RIs thus estimated are collocated against GMI-DPR rainfall to establish a regression equation between them (Fig. 1b). We have classified the precipitation spectrum (and corresponding brightness temperature and rain index) into 6 bins. These precipitation bins are defined as 2 mm/h, 8 mm/h, 15 mm/h, 20 mm/h, 25 mm/h and 30 mm/h. Figure 1c shows that histogram of number of occurrences of these bins.

It can be seen from Figure 1b that there are large scatters between rainfall and rain index which is attributed to various factors ranging from uncertainty caused by use of different sensors from different platforms (difference in viewing geometry from MFG and GPM), collocation errors, poor relationship between warm rain (light rain) and IR brightness temperature, and weak characterization of orographic rain from IR signature.

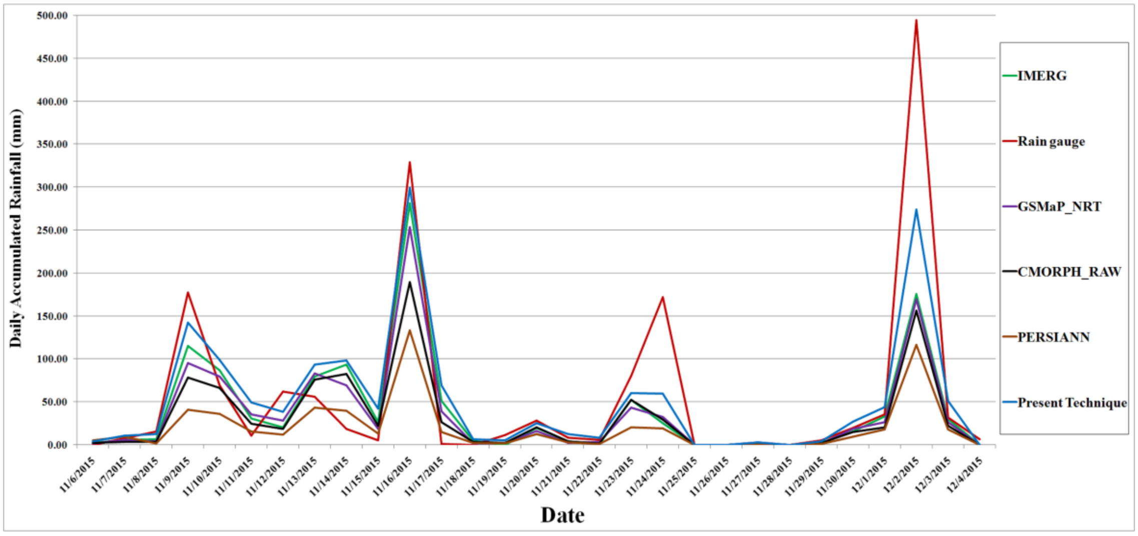

Figure 2: Rainfall over Tambram from Rain gauge, IMERG, GSMaP, CMORPH, PERSIANN and present technique during floods of 2015.

Following equation is established between RI and rain rate:

Rain rate (mm/h)= a + (b × RI^c) (4)

Where a = -3.79 (mm/h),

b = 4.55 (mm/h), and

c = 6.68.

Coefficients 'a' and 'b' essentially characterize the relationship between rain rate and rain index, allowing for variation caused by scatter in rain rate and rain index. This relationship exhibits a Correlation Coefficients (CC) of 0.83, and Standard error of estimates of 6.20 mm/h. This relationship confirms the power law relationship between rain index and rainfall as observed by past researches (Mishra et al., 2009a; Mishra 2013). RI ranges from 0.86 to 1.37. It can be concluded from figure 1b that RI>1.3 indicates heavy rainfall cases 25 mm/h and above (observation of line of fit indicated by pink color in Figure 1b).

4. Results and Discussion

Aim of the present algorithm is to monitor near real time heavy rainy systems. Performance of this technique was tested by applying it to few flood events. We have used rain gauge observation over Tamil Nadu for validation of present algorithm during flood event of Tamil Nadu in 2015.

Tamil Nadu witnessed heavy flooding during November- December in 2015. A case study has been performed for Tambram region (12.933ºN, 80.216ºE) of Kancheepuram district in Tamil Nadu during the severe flood events of 2015. For this purpose daily rainfall data from regional meteorological centre, Chennai has been used. Rain gauge based daily rainfall is estimated by accumulating rainfall in 24 hours ending 08:30 IST (03:00 GMT). For this validation purpose, hourly rainfall from IMERG, GSMaP_NRT, CMORPH_RAW, PERSIANN is accumulated in starting at 03:00 GMT of the previous day to 03:00 GMT of the day named.

It can be seen that satellite estimates underestimate heavy rainfall. Among satellite estimates, present technique is closest to rain gauge observations for monitoring heavy rainfall.

5. Conclusions

Present study merges rainfall information from combined GMI-DPR with Meteosat observations by using the high accuracy of GMI-DPR based rainfall estimates and continuous Meteosat observations to monitor heavy precipitation. It offers an opportunity to explore the climatic aspect of heavy precipitation at finer scale since MFG has long past records. Studies suggest that being able to monitor extreme rainfall at finer resolution would be sufficient to monitor flash flood (Mishra and Srinivasan 2013; Mishra 2015). Present algorithm monitors near real time heavy rainfall which is very crucial for near real time flash flood monitoring. Worldwide there is extensive requirement of near real time precipitation information for its use in hydrology and flash flood monitoring (Rafiq and Mishra 2016). Methodology proposed in the present algorithm finds application in operational contests where GEO IR data are available in near real time.

Acknowledgements

We acknowledge the funding for this work from ISRO under grant No. B. 19012/174/2016-Sec.2. Meteosat data from EUMETSET and GPM data used in this study is also thankfully acknowledged.

References

Adler, R. F., and Negri, A. J., 1988: A satellite infrared technique to estimate tropical convective and stratiform rainfall. Journal of Applied Meteorology, 27(1), 30-51.

Aonashi, K., Awaka, J., Hirose, M., Kozu, T., Kubota, T., Liu, G., Shige, S., Kida, S., Seto, S., Takahashi, N., Takayabu, Y. N., 2010: GSMaP passive microwave precipitation retrieval algorithm: Algorithm description and validation. J. Meteorol. Soc. of Japan, 87A, 119–136. doi:10.2151/jmsj.87A.119.

Grecu, M., Olson, W. S., Shie, C. L., L'Ecuyer, T. S., and Tao, W. K., 2009: Combining Satellite Microwave Radiometer and Radar observations to estimate atmospheric heating profiles. Journal of Climate, 22(23),6356-6376.

Grecu, M., and coauthors 2016: The GPM Combined Algorithm, Journal of Atmospheric and Oceanic Technology, in press, JTECH-D-16-0019.1. doi: 10.1175/JTECH-D-16-0019.1.

Huffman, G. J., Adler, R. F., Bolvin, D. T., Gu, G., Nelkin, E. J., Bowman, K. P., Hong, Y., Stocker, E. F., Wolff, D. B., 2007: The TRMM Multisatellite Precipitation Analysis (TMPA): Quasi-global, multiyear, combined-sensor precipitation estimates at fine scales. J. Hydrometeorol, 8, 38–55. doi:10.1175/ JHM560.1.

Huffman, G. J., and coauthors 2015: NASA Global Precipitation Measurement (GPM) Integrated Multi-satellitE Retrievals for GPM (IMERG), Algorithm Theoretical Basis Document (ATBD) Version 4.5, NASA, https://pmm.nasa.gov/sites/default/files/document_files/IMERG_ATBD_V4.5_0.pdf.

Iguchi, T., Kozu, T., Kwiatkowski, J., Meneghini, R., Awaka, J., & Okamoto, K. I., 2009: Uncertainties in the Rain Profiling Algorithm for the TRMM Precipitation Radar. Journal of the Meteorological Society of Japan, 87, 1-30.

Joyce, R. J., Janowiak, J. E., Arkin, P. A., and Xie, P., 2004: CMORPH: A method that produces global precipitation estimates from passive microwave and infrared data at high spatial and temporal resolution. J. Hydromet, 5, 487-503.

Kubota, T., Shige, S., Hashizume, H., Aonashi, A., Takahashi, N., Seto, S., Hirose, M., Takayabu, Y. N., Ushio, T., Nakagawa, K., Iwanami, K., Kachi, M., Okamoto, K., 2007: Global precipitation map using satellite-borne microwave radiometers by the GSMaP project: Production and validation. IEEE T. Geosci. Remote, 45, 2259–2275.

Laughlin, C. R., 1981: On the effect of temporal sampling on the observation of mean rainfall, Precipitation measurements from space. Workshop report, edited by D. Atlas and O. W.

Thiele, pp. D59–D66, NASA/Goddard Space Flight Cent., Greenbelt, Md.

Mishra, A., 2012: Estimation of heavy rainfall during cyclonic storms from microwave observations using nonlinear approach over Indian Ocean. Natural Hazards, 63, 673-683. DOI 10.1007/s1 1069-012-0179-4.

Mishra, A., 2015: A study on the occurrence of flood events over Jammu and Kashmir during September 2014 using satellite remote sensing. Natural Hazards, 78, 1463-1467.

Mishra, A., and Srinivasan, J., 2013: Did a cloud burst occur in Kedarnath during 16 and 17 June 2013?. Current Science, 105(10),1351-1352.

Mishra, A., Gairola, R. M., Varma, A. K., Sarkar, A., and Agarwal, V. K., 2009a: Rainfall Retrieval over Indian land and oceanic regions from SSM/I Microwave data. Advances in Space research, 44,815-823.

Mishra, A., Gairola, R. M., Varma, A. K., & Agarwal, V. K., 2009b: Study of Intense Heavy Rainfall Events over India Using KALPANA-IR and TRMM- Precipitation Radar Observations. Current Science, 9(5), 689-695.

Mishra, A., Gairola, R. M., Agarwal, V. K., 2011a: Rainfall Estimation from combined observations using KALPAANA-IR and TRMM-Precipitation Radar measurements over Indian Region. Journal of Indian Society of Remote Sensing, 40(1), 65-74.

Mishra, A., Gairola, R. M., Varma, A. K., Agarwal, V. K., 2011b: Improved rainfall estimation over Indian land oceanic regions using satellite infrared technique. Advances in Space research, 48: 49-55. doi: 10.1016/j.asr.2011.02.016.

Mishra, A., Gairola, R. M., Varma, A. K., and Agarwal, V. K., 2010: Remote sensing of Precipitation over Indian land and oceanic regions by synergistic use of multi-satellite sensors. Journal of Geophysical Research, 115, D08106. doi no. 10.1029/2009JD012157.

Mishra, A., 2013: A new technique to estimate precipitation at fine scale using multifrequency satellite observations over Indian land and oceanic regions. IEEE Transactions on Geoscience and Remote Sensing, 51(7), 4349-4358.

Mishra, A.K., 2012: Estimation of heavy rainfall during cyclonic storms from microwave observations using nonlinear approach over Indian Ocean. Natural hazards, 63(2), 673-683.

Mishra, A. and Rafiq, M., 2017. Towards combining GPM and MFG observations to monitor near real time heavy precipitation at fine scale over India and nearby oceanic regions. Dynamics of Atmospheres and Oceans, 80, pp.62-74.

Mishra, A., Chandra, S., Rafiq, M., Sivarajan, N. and Santhanam, K., 2018. An observational study of the Kanchipuram flood during the northeast monsoon season in 2015. Weather. doi.org/10.1002/wea.3271

Rafiq, M., & Mishra, A. K., 2018a. Remote Sensing of Near-Real-Time Heavy Precipitation Using Observations from GPM and MFG over India and Nearby Oceanic Regions. In Multidisciplinary Digital Publishing Institute Proceedings (Vol. 2, No. 7, p. 327).

Rafiq, M. and Mishra, A.K., 2018b. A study of heavy snowfall in Kashmir, India in January 2017. Weather, 73(1), pp.15-17.

Rafiq, M. and Mishra, A., 2016. Investigating changes in Himalayan glacier in warming environment: a case study of Kolahoi glacier. Environmental Earth Sciences, 75(23), p.1469.

Rao, B. D. V., Hari Prasad, D., and Srinivas, D., 2009: Impact of horizontal resolution and the advantages of the nested domains approach in the prediction of tropical cyclone intensification and movement. J. Geophys. Res, 114, D11106. doi:10.1029/2008JD011623.

Roca, R., Viollier, M., Picon, L., and Desbois, M., 2002: A multisatellite analysis of deep convection and its moist environment over the Indian Ocean during the winter monsoon. Journal of geophysical research, 107, (D19). doi: 10.1029/2000JD000040.

Rosenfeld, D., & Gutman, G., 1994: Retrieving microphysical properties near the tops of potential rain clouds by multispectral analysis of AVHRR data. Atmospheric research, 34(1), 259-283.

Scofield, R. A., and Kuligowski, R. J., 2003: Status and outlook of operational satellite precipitation algorithms for extreme-precipitation events. Mon. Wea. Rev, 18,1037-1051.